JOURNAL OF SOLID STATE CHEMISTRY 108, 46–50 (1993)

# A Molybdenum (V) Diphosphate Closely Related to the $\alpha$-$NaTiP_2O_7$ Structure: $Cs(MoO)P_2O_7$

A. Guesdon, M. M. Borel, A. Leclaire, A. Grandin, and B. Raveau

*Laboratoire CRISMAT ISMRA/Université de Caen, Boulevard du Maréchal Juin, 14050 Caen Cedex, France*

Received December 29, 1992; in revised form April 16, 1993; accepted April 20, 1993

A new Mo(V) diphosphate $Cs(MoO)P_2O_7$ with a tunnel structure has been isolated. It crystallizes in the space group $P2_1/n$ with $a = 5.134$ Å, $b = 11.707$ Å, $c = 12.063$ Å, $\beta = 91.77°$. The $[MoP_2O_8]_\infty$ framework consists of $[MoP_2O_{11}]_\infty$ chains waving along b and c and built up of corner-sharing $P_2O_7$ groups and $MoO_6$ octahedra, like in $K(MoO)P_2O_7$. The two structures $K(MoO)P_2O_7$ and $Cs(MoO)P_2O_7$ differ by the configuration of their $P_2O_7$ groups which are eclipsed and staggered respectively. In fact, this structure is closely related to that of $\alpha$-$NaTiP_2O_7$. It is built up similarly of layers of diphosphate groups and of $MoO_6$ octahedra stacked along b and forming similar hexagonal tunnels running along [101] and [$\bar{1}$01]. This structure differs from that of $\alpha$-$NaTiP_2O_7$ by the staggered configuration of its $P_2O_7$ groups leading to different orientation of the $MoO_6$ octahedra between two successive octahedral layers, and by the fact that some $P_2O_7$ groups and $MoO_6$ are disconnected. 

## INTRODUCTION

The investigation of pentavalent molybdenum phosphates, performed these last years, have allowed about twenty new compounds to be synthesized with various structures, whose relationships have recently been studied (1). The particular geometry of the $MoO_6$ octahedra, characterized by a molybdenyl ion and a free apex, allows open structures to be generated, in which large cations can be interpolated. This is the case of the diphosphate $K(MoO)P_2O_7$ (2) which is isotypic with the niobium phosphate $K(NbO)P_2O_7$ (3) in spite of the different electronic configurations of Nb(V) and Mo(V). From the existence for $CsNbP_2O_8$ of two different original layer structures, $Cs(NbO)P_2O_7$ (4) and $CsNb(PO_4)_2$ (5), raises the issue of the possible synthesis of molybdenum (V) analogous phases. We report here on the crystal structure of a new Mo(V) diphosphate $Cs(MoO)P_2O_7$, whose original framework is closely related to that of $\alpha$-$NaTiP_2O_7$ (6) and exhibits also some similarity with $K(MoO)P_2O_7$.

## SYNTHESIS

Single crystals of the Mo(V) phosphate were grown from a mixture of nominal composition "$CsMoP_2O_8$." First $H(NH_4)_2PO_4$, $Cs_2CO_3$, and $MoO_3$ were mixed in an agate mortar in adequate ratios according to the composition "$CsMo_{0.833}P_2O_8$" and heated at 600 K in a platinum crucible to decompose the ammonium phosphate and carbonate. In a second step, the resulting mixture was then added to the required amount of molybdenum (0.166 mole), placed in an alumina tube and sealed in an evacuated silica ampoule, then heated for one day at 1023 K and cooled to 2 K per hour down to 923 K. The sample was finally quenched to room temperature.

Yellow crystals corresponding to $Cs(MoO)P_2O_7$ were extracted from the resulting product. Their composition was also confirmed by microprobe analysis. Subsequently, a reaction to prepare pure powder of $Cs(MoO)P_2O_7$ was carried out at 950 K for 12 hr and quenched to room temperature. The powder X-ray diffraction pattern (Table 1) of this phosphate was indexed in a monoclinic cell (Table 2) in agreement with the parameters obtained from the single crystal X-ray study.

In spite of the unit-cell dimensions and space group, similar to those of $K(MoO)P_2O_7$, $Cs(MoO)P_2O_7$ exhibits very different powder X-ray pattern which suggests a fundamentally different structure.

## STRUCTURE DETERMINATION

A yellow crystal, with dimensions $0.077 \times 0.026 \times 0.026$ mm$^3$, was selected for the structure determination. The cell parameters reported in Table 2 were determined and refined by diffractometric techniques at 294 K with a least squares refinement based upon 25 reflections with $18 < \theta < 22°$. The data were collected on a CAD4 Enraf-Nonius diffractometer with the data collection parameters of Table 2. The reflections were corrected for Lo-



0022-4596/94 $6.00

TABLE 1
Interreticular Distances

| $h$ | $k$ | $l$ | $d_{cal}$ Å | $d_{obs}$ Å | $I$ | $h$ | $k$ | $l$ | $d_{cal}$ Å | $d_{obs}$ Å | $I$ |
|---|---|---|---|---|---|---|---|---|---|---|---|
| 0 | 1 | 1 | 8.399 | 8.365 | 5 | 0 | 4 | 1 | 2.844 | 2.843 | 4 |
| 0 | 2 | 0 | 5.854 | 5.841 | 7 | 1 | 3 | 2 | 2.740 | 2.740 | 4 |
| 0 | 1 | 2 | 5.360 | 5.478 | 7 | 0 | 2 | 4 | 2.680 | 2.675 | 4 |
| 0 | 2 | $\bar{1}$ | 5.266 | 5.257 | 20 | 0 | 4 | 2 | 2.633 | 2.624 | 20 |
| 1 | 1 | $\bar{1}$ | 4.421 | 4.422 | 5 | 1 | 4 | 0 | 2.542 | 2.551 | 18 |
| 0 | 2 | 2 | 4.200 | 4.198 | 43 | 1 | 4 | $\bar{1}$ | 2.495 | 2.492 | 10 |
| 1 | 2 | 0 | 3.859 | 3.859 | 54 | 1 | 4 | 1 | 2.480 | 2.476 | 10 |
| 0 | 1 | $\bar{3}$ | 3.801 | 3.800 | 64 | 0 | 3 | $\bar{4}$ | 2.385 | 2.382 | 20 |
| 1 | 1 | $\bar{2}$ | 3.759 | 3.750 | 14 | 2 | 2 | $\bar{1}$ | 2.319 | 2.317 | 22 |
| 0 | 3 | 1 | 3.713 | 3.709 | 100 | 2 | 1 | 2 | 2.290 | 2.285 | 4 |
| 1 | 1 | 2 | 3.657 | 3.651 | 48 | 0 | 2 | 5 | 2.230 | 2.227 | 10 |
| 1 | 2 | 1 | 3.651 | | | 1 | 0 | $\bar{5}$ | 2.209 | 2.207 | 10 |
| 0 | 2 | $\bar{3}$ | 3.313 | 3.312 | 97 | 1 | 3 | $\bar{4}$ | 2.184 | 2.180 | 15 |
| 1 | 2 | $\bar{2}$ | 3.285 | 3.280 | 7 | 0 | 5 | 2 | 2.183 | | |
| 0 | 3 | 2 | 3.276 | | | 2 | 2 | 2 | 2.169 | 2.168 | 2 |
| 1 | 2 | $\bar{2}$ | 3.216 | 3.215 | 29 | 1 | 0 | $\bar{5}$ | 2.157 | 2.157 | 3 |
| 1 | 0 | $\bar{3}$ | 3.213 | | | 2 | 1 | $\bar{3}$ | 2.156 | | |
| 1 | 0 | 3 | 3.118 | 3.116 | 20 | 1 | 3 | 4 | 2.143 | 2.142 | 6 |
| 1 | 3 | 0 | 3.106 | 3.100 | 21 | 1 | 1 | 5 | 2.121 | 2.122 | 3 |
| 1 | 1 | $\bar{3}$ | 3.098 | | | 2 | 1 | 3 | 2.098 | 2.097 | 3 |
| 0 | 0 | 4 | 3.014 | 3.012 | 18 | 0 | 3 | 5 | 2.051 | 2.051 | 2 |
| 1 | 1 | 3 | 3.013 | | | 1 | 2 | 5 | 2.024 | 2.024 | 2 |
| 0 | 4 | 0 | 2.927 | 2.922 | 21 | 0 | 5 | 3 | 2.023 | 2.021 | 2 |
| 0 | 1 | 4 | 2.919 | | | | | | | | |

TABLE 2
Summary of Crystal Data, Intensity Measurements, and Structure Refinement Parameters for $Cs(MoO)P_2O_7$

| | | |
|---|---|---|
| | 1. Crystal data | |
| Space group | $P2_1/n$ | |
| Cell dimensions | $a$ = 5.1340(5) Å | |
| | $b$ = 11.707(2) Å | $\beta$ = 91.77(1)° |
| | $c$ = 12.063(2) Å | |
| Volume | $v$ = 724.7(3) Å$^3$ | |
| $Z$ | 4 | |
| $\rho$th | 3.84 | |
| $\rho$exp | 3.9 | |
| | 2. Intensity measurements | |
| $\lambda$ (Mo$K\alpha$) | 0.71073 Å | |
| Scan mode | $\omega$–$\theta$ | |
| Scan width (°) | 0.95 + 0.35 tn $\theta$ | |
| Slit aperture (mm) | 1.06 + tn $\theta$ | |
| Max $\theta$ (°) | 45 | |
| Standard reflections | 3 every 3000 sec (no decay) | |
| Reflections with $I > 3\sigma$ | 797 | |
| Reflections measured | 6339 | |
| | 3. Structure solution and refinement | |
| Parameters refined | 70 | |
| Agreement factors | $R$ = 0.035 | $R_W$ = 0.034 |
| Weighting scheme | $w = f(\sin\theta/\lambda)$ | |
| $\Delta/\sigma$ max | <0.004 | |

TABLE 3
Positional Parameters and Their Estimated Standard Deviations in Pararentheses

| Atom | $x$ | $y$ | $z$ | $B$(Å)$^2$ |
|---|---|---|---|---|
| Mo | 0.2365(2) | 0.04536(9) | 0.18973(9) | 0.58(1) |
| Cs | 0.7688(2) | 0.33667(8) | 0.05123(8) | 1.78(1) |
| P(1) | 0.7646(6) | 0.1668(3) | 0.3101(3) | 0.77(5) |
| P(2) | 0.7781(6) | 0.3972(2) | 0.4185(3) | 0.57(5) |
| O(1) | 0.238(2) | −0.0362(8) | 0.3029(8) | 1.6(1)* |
| O(2) | 0.026(1) | 0.1750(7) | 0.2542(7) | 0.8(1)* |
| O(3) | 0.551(2) | 0.1379(7) | 0.2233(7) | 1.1(1)* |
| O(4) | −0.097(2) | −0.0083(7) | 0.1164(7) | 0.8(1)* |
| O(5) | 0.440(2) | −0.0717(6) | 0.1000(7) | 0.8(1)* |
| O(6) | 0.247(1) | 0.1455(6) | 0.0339(6) | 0.6(1)* |
| O(7) | 0.763(2) | 0.0989(8) | 0.4119(8) | 1.6(2)* |
| O(8) | 0.699(2) | 0.2986(7) | 0.3341(7) | 1.0(1)* |

*Note.* Starred atoms were refined isotropically. Anisotropically refined atoms are given in the form of the isotropic equivalent displacement parameter defined as:

$$B = \frac{4}{3}\sum_i \sum_j \mathbf{a}_i \cdot \mathbf{a}_j \cdot \beta_{ij}.$$

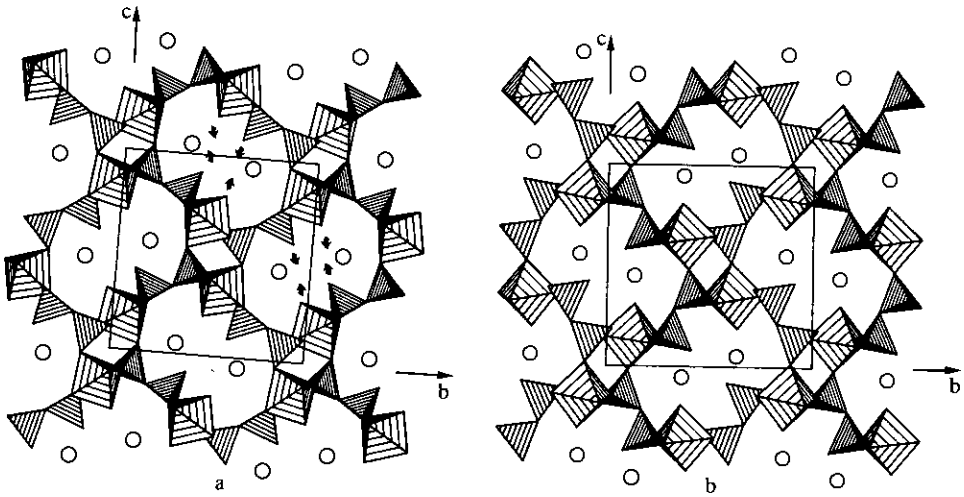


FIG. 1. (a) Projection of $Cs(MoO)P_2O_7$ along **a**, (b) Projection of $K(MoO)P_2O_7$ along **a** showing the orientation of the $P_2O_7$ groups and of the tunnels which are different in the two compounds.

rentz, polarization, and absorption (Gaussian method) effects. The Patterson function, different from that of $K(MoO)P_2O_7$, confirms the nonisotypy of the two compounds.

Atomic coordinates of the molybdenum atom were deduced from the Patterson function and the other atoms were located by subsequent Fourier series.

The insufficient number of reflection with $I > 3\sigma(I)$ does not allow to refine anisotropic thermal factors for the oxygen atoms. Refinement of the atomic coordinates and their thermal parameters led to $R = 0.035$ and $R_W = 0.034$ and to the atomic parameters of Table 3.

## DESCRIPTION OF THE STRUCTURE AND DISCUSSION

The projection of the structure of this new diphosphate onto (100) (Fig. 1a) compared with that of $K(MoO)P_2O_7$ (Fig. 1b) shows that both $[MoP_2O_8]_\infty$ frameworks consist of corner-sharing $MoO_6$ octahedra and $P_2O_7$ groups forming large tunnels running along **a** where the $Cs^+$ or $K^+$ cations are located. In both frameworks, each octahedron is linked to five $P_2O_7$ groups and has one free apex, and reciprocally each $P_2O_7$ group shares five corners with $MoO_6$ octahedra and has one free corner. However, the two structures are basically different in spite of the similarity of their cell parameters and of their identical space group, $P2_1/n$. Indeed, it can be seen that the tunnels are different, by their orientation and also by their shape. The two frameworks can be simply described from the simple assemblage of $[MoP_2O_{11}]_\infty$ waving chains running either along **b** or along **c** (Figs. 2a and 2b). As shown in Figure 2, the difference between these two chains deals in the different orientation of the $P_2O_7$ groups. While in $K(MoO)P_2O_7$, the $P_2O_7$ groups are staggered, they are

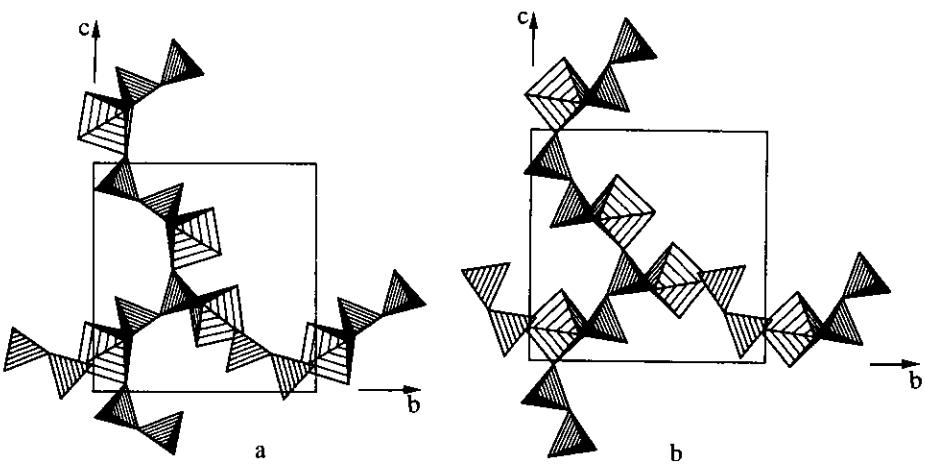


FIG. 2. $[MoP_2O_{11}]_\infty$ waving chains running along **b** and **c**. (a) in $Cs(MoO)P_2O_7$, (b) in $K(MoO)P_2O_7$. The main difference in the two chains is the sitting of the free apices of $P_2O_7$.

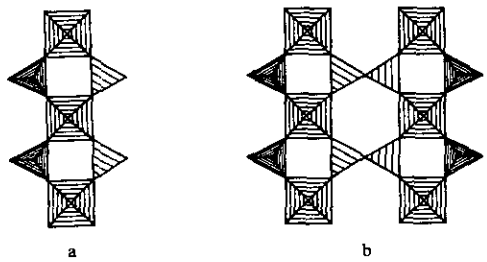


FIG. 3. $Cs(MoO)P_2O_7$: (a) $[MoP_2O_{10}]_\infty$ column, (b) two chains share the apices of their tetrahedra, forming eclipsed $P_2O_7$ groups.

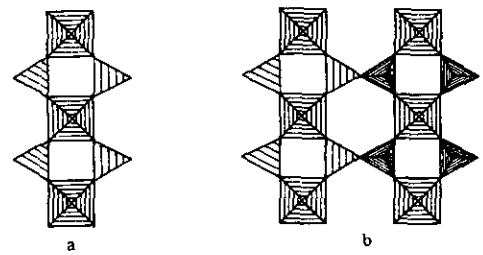


FIG. 4. $K(MoO)P_2O_7$: (a) $[MoP_2O_{10}]_\infty$ column, (b) two chains share the apices of their tetrahedra, forming staggered $P_2O_7$ groups.

eclipsed in the $Cs(MoO)P_2O_7$ structure. It is this difference between the conformation of the $P_2O_7$ groups which is at the origin of the difference between the two $[MoP_2O_8]_\infty$ frameworks. Indeed, both structures are built up from $[MoP_2O_{10}]_\infty$ columns running along **a**, but in these columns the $PO_4$ tetrahedra point their fourth corner along **c** in two opposite directions in $Cs(MoO)P_2O_7$ (Fig. 3a), whereas they are all oriented in the same direction in $K(MoO)P_2O_7$ (Fig. 4a); then the association of two $[MoP_2O_{10}]_\infty$ chains leads to eclipsed $P_2O_7$ groups in $Cs(MoO)P_2O_7$ (Fig. 3b), whereas staggered groups are obtained in $K(MoO)P_2O_7$ (Fig. 4b).

In fact, the projection of this structure along **c** (Fig. 5a), compared to the projection of $\alpha$-$NaTiP_2O_7$ along **a** (Fig. 5b), shows that both frameworks, $[MoP_2O_8]_\infty$ and $[TiP_2O_7]_\infty$, are very closely related. Both structures consist of the alternative stacking of layers of $P_2O_7$ groups with layers of $MoO_6$ octahedra along **b** in $MoOP_2O_7$ and with layers of $TiO_6$ octahedra along **c** in $\alpha$-$NaTiP_2O_7$. As a result one observes hexagonal tunnels running along [101] and [$\bar{1}$01] as shown from the projection of the structure along these directions (Fig. 6a), which are very similar to those running along [100] or [110] in $\alpha$-$NaTiP_2O_7$ (Fig. 6b). However, the $[MoP_2O_8]_\infty$ framework differs from the $[TiP_2O_7]_\infty$ host lattice by the conformation of its $P_2O_7$ groups which are eclipsed, whereas they are staggered in $\alpha$-$NaTiP_2O_7$. Consequently two successive (001) octahedral layers are turned of approximately 60° in $\alpha$-$NaTiP_2O_7$ whereas the octahedra of two successive (100) octahedral layers in $Cs(MoO)P_2O_7$ are almost above each other. One also recognizes, from the (100) projection (Fig. 1a) that the structure consists of (100) layers of diphosphate groups which alternate with layers of $MoO_6$ octahedra as in $\alpha$-$NaTiP_2O_7$. Note that in the latter projection some $P_2O_7$ groups and $MoO_6$ octahedra are disconnected (see arrows); their connection would lead to a $[MoP_2O_7]_\infty$ framework with hexagonal tunnels running along **a** and similar to these observed in $\alpha$-$NaTiP_2O_7$.

The geometry of the $PO_4$ tetrahedra is characteristic of the $P_2O_7$ groups with three short distances (1.46–1.52 Å) (Table 4) corresponding either to P–O–Mo bonds or to the nonbonded oxygen and a longer one (1.58–1.60 Å) corresponding to the bridging bond P–O–P.

The geometry of the $MoO_6$ octahedron is characteristic of Mo(V), i.e., very similar to that observed in other Mo(V) phosphates. The "$O_6$" octahedron containing Mo is almost regular (Table 4), but the molybdenum atom is off-centered out of its basal plane of 0.256 Å towards the unshared oxygen O(1), leading to very short Mo–O distance of 1.67 Å. The four Mo–O distances of the basal plane exhibit intermediate values ranging 1.978 to 2.053 Å, whereas the sixth Mo–O bond, opposite to the

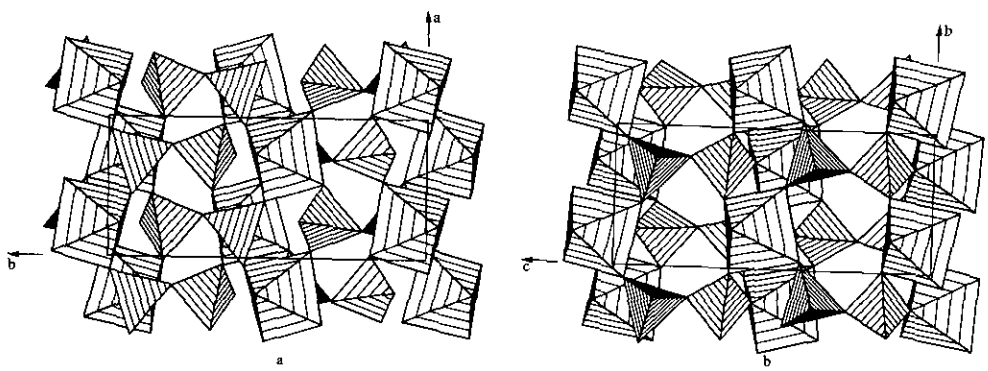


FIG. 5. (a) Projection of $Cs(MoO)P_2O_7$ along **c**, (b) Projection of $\alpha$-$NaTiP_2O_7$ along **a**.

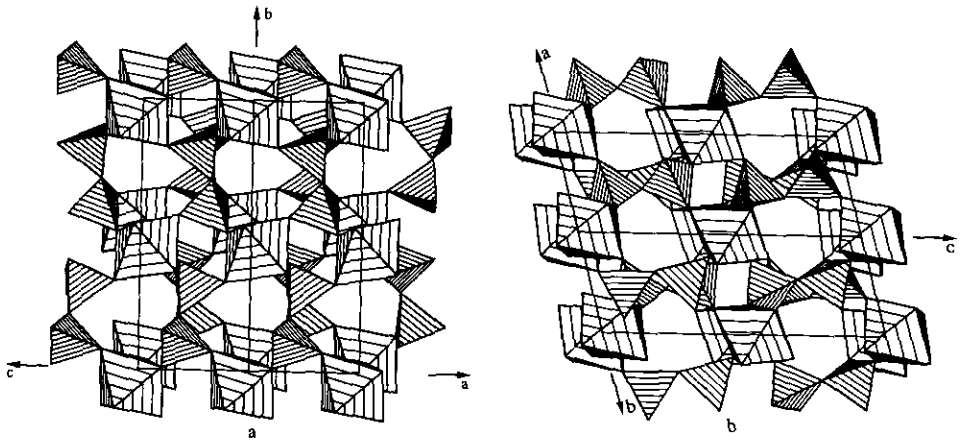


FIG. 6. (a) Projection of $Cs(MoO)P_2O_7$ along [101], (b) Projection of $\alpha$-$NaTiP_2O_7$ along [110].

short molybdenyl bond, is significantly larger (2.218 Å). This configuration is also observed in $K(MoO)P_2O_7$, with similar distances.

TABLE 4
Distances (Å) And Angles (°) in the Polyhedra

| Mo | O(1) | O(2) | O(3) | O(4) | O(5) | O(6) |
|---|---|---|---|---|---|---|
| O(1) | 1.67(1) | 2.76(1) | 2.79(1) | 2.81(1) | 2.72(1) | 3.88(1) |
| O(2) | 95.9(4) | 2.032(8) | 2.77(1) | 2.77(1) | 3.45(1) | 2.94(1) |
| O(3) | 99.5(4) | 87.4(3) | 1.978(8) | 2.83(1) | 2.92(1) | 2.73(1) |
| O(4) | 99.4(4) | 86.9(3) | 160.8(3) | 2.004(8) | 2.87(1) | 2.73(1) |
| O(5) | 93.5(4) | 170.5(3) | 92.7(3) | 90.0(3) | 2.053(8) | 2.84(1) |
| O(6) | 176.6(4) | 87.5(3) | 80.9(3) | 80.5(3) | 83.1(3) | 2.218(8) |

| P(1) | O(2$^{ii}$) | O(3) | O(7) | O(8) |
|---|---|---|---|---|
| O(2$^{ii}$) | 1.523(8) | 2.49(1) | 2.53(1) | 2.44(1) |
| O(3) | 109.4(5) | 1.529(9) | 2.53(1) | 2.42(1) |
| O(7) | 115.8(5) | 115.6(5) | 1.46(1) | 2.54(1) |
| O(8) | 102.2(5) | 100.7(5) | 111.3(5) | 1.608(9) |

| P(2) | O(4$^{v}$) | O(5$^{i}$) | O(6$^{vi}$) | O(8) |
|---|---|---|---|---|
| O(4$^{v}$) | 1.497(9) | 2.49(1) | 2.53(1) | 2.40(1) |
| O(5$^{i}$) | 11.6(5) | 1.515(8) | 2.47(1) | 2.51(1) |
| O(6$^{vi}$) | 115.3(5) | 110.3(5) | 1.492(8) | 2.50(1) |
| O(8) | 102.3(5) | 107.9(5) | 108.8(5) | 1.584(9) |

Cs–O(1$^{i}$) = 3.385(10)
Cs–O(2$^{ii}$) = 3.335(8)
Cs–O(3) = 3.334(9)
Cs–O(6) = 3.491(8)
Cs–O(6$^{ii}$) = 3.334(8)
Cs–O(7$^{iii}$) = 3.142(9)
Cs–O(7$^{i}$) = 3.176(10)
Cs–O(7$^{iv}$) = 3.106(9)
Cs–O(8) = 3.471(9)

Symmetry code
i: $\frac{3}{2} - x, \frac{1}{2} + y, \frac{1}{2} - z$,
ii: $1 + x, y, z$
iii: $-\frac{1}{2} + x, \frac{1}{2} - y, -\frac{1}{2} + z$,
iv: $\frac{1}{2} + x, \frac{1}{2} - y, -\frac{1}{2} + z$,
v: $\frac{1}{2} - x, \frac{1}{2} + y, \frac{1}{2} - z$,
vi: $\frac{1}{2} + x, \frac{1}{2} - y, \frac{1}{2} + z$,

The cesium cations, located in the large tunnels parallel to **a** are surrounded by nine oxygen atoms at distances ranging from 3.10 to 3.491 Å.

## CONCLUDING REMARKS

This study illustrates once again the great variety of the mixed frameworks built up from $MoO_6$ octahedra and $PO_4$ tetrahedra and involving Mo(V). This behavior results from the ability of the Mo(V) octahedra to present a free apex, leading to a larger flexibility of the structure, enhanced by the different configurations adopted by the $P_2O_7$ groups, from staggered to eclipsed. This suggests that cations larger than cesium, such as alkylammonium ions, should allow open structures with zeolithic properties to be prepared in these systems, using hydrothermal synthesis techniques.

## REFERENCES

1. G. Costentin, A. Leclaire, M. M. Borel, A. Grandin, and B. Raveau, *Inorg. Rev.* in press.
2. C. Gueho, M. M. Borel, A. Grandin, A. Leclaire, and B. Raveau, *Z. Anorg. Allg. Chem.* **615,** 104 (1992).
3. S. A. Linde, Yu. E. Gorbunova, A. V. Lavrov, and I. V. Tananaev, *Dokl. Akad. Nauk. SSSR* **250,** 96 (1980).
4. V. P. Nikolaev, G. G. Sadikov, A. V. Lavrov, and M. A. Porai-Koshits, *Dokl. Akad. Nauk SSSR* **264,** 859 (1982).
5. S. Oyetola, A. Verbaere, Y. Piffard, and M. Tournoux, *Eur. J. Solid State Inorg. Chem.* **25,** 259 (1988).
6. A. Leclaire, A. Benmoussa, M. M. Borel, A. Grandin, and B. Raveau, *J. Solid State Chem.* **77,** 299 (1988).